Crystallinity and Disorder in Poly(ethylene Terephthalate) Fibers. Specific Example of Preoriented Yarns (POY)

MICHEL SOTTON, ANNE-MARIE ARNIAUD, and CHRISTIANE RABOURDIN, *Laboratory of the French Textile Institute, 92100 Boulogne sur Seine, France*

Synopsis

Crystallinity measurements were carried out on PET fibers following Ruland's method, taking into account an isotropic disorder parameter, and the "relative method" which is used for routine controls. Two extreme kinds of samples were studied: relatively crystallized industrial yarns (tire cords) with different abilities of shrinkage and annealed without tension, and preoriented yarns (POY) of very low crystallinity, produced at speeds of 1000–4000 m/min. Special care was taken during the experimental work—for sample preparation, monochromatization of the x-ray beam, corrections of intensity values, drawing of the background. In this way it was possible to find an excellent correlation between crystallinities measured by Ruland's calculations and indexes of crystallinity obtained by the relative method. There is a large increase of crystallinity in heat-treated samples when a strong shrinkage is allowed. In this case the disorder parameter which is specific of the crystalline phase is also increased. There is only a slight increase in the crystalline fraction in stabilized samples (little or no ability to shrink) when annealed, but an improvement of the order of the crystalline areas. Nevertheless it appears impossible to improve the order of the crystallites in shrunk fiber above a "critical value," even if extended heat treatments are carried out. There is a small crystalline fraction in POY produced at 3000–3300 m/min; these "crystalline nuclei" are characterized by their very low disorder parameter (thermal disorder). In order to estimate the mesophase in POY x-ray patterns, an attempt was made to draw the boundary between peaks and background, following two references: first, an "amorphous fiber" x-ray diagram, then a "calculated true amorphous" one. It was shown that the estimated mesophase fraction in low-oriented yarns (spinning speed 1000–2500 m/min) progressively decreases at the benefit of a crystalline area when production speed increases.

INTRODUCTION

There is no doubt that the results of the first studies carried out by x-ray diffractometry on natural or artificial fibers contributed much to the development of the structural models which, apart from some slight changes, are still used for the understanding of the structure properties of modern man-made fibers.

The choice made in relation to the idea of a two-phase fibrillar structure with a more or less accentuated separation between the crystalline and amorphous parts explains the interest of the research workers in their effort to determine methods of calculation for this crystalline fraction responsible for the diffraction of x-rays. The appearance of new investigation techniques and their application in the study of fibrous materials have led to other parameters linked with crystallinity (crystallinity by IR spectrography, NMR, neutron diffusion, DSC, etc.) and more or less correlated to that measured by x-ray diffraction. Such divergences linked with the specificity of each technique and of the relative structural level should be used for a better knowledge of the structure of fibrous materials

Journal of Applied Polymer Science, Vol. 22, 2585–2608 (1978)

0021-8995/78/0022-2585$01.00

and eventually for the proposal of more elaborate models than the conventional two-phase one. Attempts have already been made in this respect either taking into account only the results of x-ray diffraction[1,2] or in combining the results obtained by x-ray diffractometry and infrared spectrography.[3]

In another connection, formulations have been proposed for a long time[4] for the characterization of each phase and which take into consideration the parameters of orientation and crystallinity. It is obvious that with this approach to the problem, each parameter should be treated with the utmost care; and the present work has for its objective a better definition of the "crystalline fraction" of polyester fibers measured according to an x-ray diagram. The methods generally employed are based on the separation between crystalline peaks and background noise, but they do not take into account the thermal and structural disorders which increase the background noise and therefore lead to the underestimation of the crystalline fraction. Johnson et al. have tried recently to redefine the method of calculating the crystallinity of fibrous materials in specifying a disorder parameter.[5,6] In order to do this, the individual profiles have to be calculated by formulating certain hypotheses on their form and their angular position. This theoretical approach only employed at present on the paratropic interferences cannot be easily applied to the large angular intervals when the number of peaks is important; this is precisely the case when examinations are carried out on samples in which the orientation of structural elements is a random one.

The method for calculating the degree of crystallinity in polymers proposed by Ruland[7] and considered again in a more simplified form by Vonk[8] and Perret[9] takes into account the scattered intensity over a wide zone of reciprocal space and enables the "apparent crystallinity" to be corrected by a disorder parameter. Such a method has been retained for the study of very crystallized cotton fibers in the diffraction diagrams of which the separation between peaks and background noise can be made without too much ambiguity.[10] The case of man-made fibers of relatively low crystallinity is a greater problem.

In the present study, carried out on semicrystalline PET fibers and on not very crystallized POY yarns, two objectives were fixed: (1) the calculation of the real crystallinity, calculation of a disorder parameter according to Ruland's method and tentative of correlation with a crystallinity index obtained according to a more simple method employed for routine control (so-called relative method); (2) estimation of an ordered mesophase fraction in yarns preorientated under the spinneret.

THEORETICAL REVIEW

Degree of Crystallinity According to Ruland's Method

The basic equations proposed by Ruland for the calculation of the crystallinity of polymers give the following results:

$$x_c = \frac{\int_0^\infty s^2 I_{cr(s)} ds}{\int_0^\infty s^2 I_{(s)} ds} \cdot \frac{\int_0^\infty s^2 \bar{f}^2 ds}{\int_0^\infty s^2 \bar{f}^2 D\, ds} \tag{1}$$

where x_c = weight fraction of the crystalline material in the polymer; $s = 2 \sin \theta/\lambda$, magnitude of the radial vector **s** in the reciprocal space (2θ = diffraction angle, λ = wavelength expressed in Å); $I_{(s)}$ = coherent scattered intensity; $I_{cr(s)}$ = part of the coherent scattering which is concentrated into the crystalline peaks; $\bar{f}^2$ = mean square of the scattering factors of the atoms in the polymer; and D = disorder function.

The originality of this method lies in the taking into account a corrective factor K of the "apparent" crystallinity, which is itself a function of a disorder parameter D:

$$K = \frac{\int_0^\infty s^2 \bar{f}^2 \, ds}{\int_0^\infty s^2 \bar{f}^2 D \, ds}$$

D comprises the disorder due to thermal motions and the lattice imperfections of first and second order. Ruland showed that these two kinds of disorder in the crystalline part of polymers could be represented approximately as one and the same function:

$$D = \exp^{-ks^2}$$

under the assumption that there is an isotropic disorder. In order to justify the use of a corrective term in calculating crystallinity, Ruland noticed that even in a completely crystalline substance scattered x-ray intensity is not exclusively localized in the diffraction peaks. Actually, because the atoms can move away from their ideal position by thermal motions or by distortions, a part of the scattered x-rays escape the peaks and is redistributed in the reciprocal space. The method of examining the diagrams consists in separating the crystalline peaks from the background noise and, because of this fact, leads to an underestimation of the polymer crystalline fraction.

In examining the samples of different crystallinity and taking into account the scattered intensity in a large region of reciprocal space, it is possible, according to Ruland, to define by experiment a certain number of integration intervals such as the equation

$$\int_{s_0}^{s_p} s^2 I_{(s)} \, ds \simeq \int_{s_0}^{s_p} s^2 \bar{f}^2 \, ds \tag{2}$$

to be verified independently from the crystallinity of the substance, s_0 and s_p being the lower and upper limits of integration intervals.

Equation (1) can therefore be used on these angular intervals for any sample under the form

$$x_c = \frac{\int_{s_0}^{s_p} s^2 I_{cr(s)} \, ds}{\int_{s_0}^{s_p} s^2 I(s) \, ds} K(s_0, s_p, D, \bar{f}^2) = C^{st} \tag{3}$$

with

$$K = \frac{\int_{s_0}^{s_p} s^2 \bar{f}^2 \, ds}{\int_{s_0}^{s_p} s^2 \bar{f}^2 \exp^{-ks^2} \, ds} \tag{4}$$

The different integration intervals having been defined, this system of equations can be resolved by calculating the nomogram of K values which maintain constant the crystallinity x_c for a given function of disorder D.

Crystallinity Index According to the Relative Method

This method was initially proposed by Wakelin[11] in order to study the crystallinity of cotton fibers and by Statton[12] for PET fibers; it consists in comparing the x-ray diagram of any sample to that of two standard samples: one being considered as 100% crystalline, the other as 100% amorphous

$$I_c = \frac{\Sigma XY - (1/n)\,\Sigma X\,\Sigma Y}{\Sigma X^2 - (1/n)\,[\Sigma X]^2}$$

where I_c = crystallinity index; X = difference of intensity observed at each angle $(2\theta)_i$ between the unknown and amorphous; and Y = difference of intensity observed at each angle $(2\theta)_i$ between amorphous and crystalline. The comparison of the diagrams is carried out after the correction and standardization of intensities. This method can otherwise be generalized and applied in the case of materials having two crystalline phases, for example mercerized cotton fibers.[13,14]

In general, the relative method adopted in routine controls only takes into consideration the crystalline peaks in a reduced angular interval of 7°–40° in 2θ. The value of the crystallinity index is obviously a function of the "quality" of the standard samples.

EXPERIMENTAL

Samples

Two kinds of samples were studied: firstly, continuous filament yarns, relatively crystallized after thermal treatments and having the following characteristics:

1. PET Filament single yarn (industrial sample): 110 tex f220 S 28 tpm (Tergal 5 dtex), shrinkage capacity 8%.
2. PET Filament single yarn (industrial sample): 116 tex f220 S 32 tpm (Tergal 5.25 dtex), stabilized sample (conditions of stabilization are unknown), residual shrinkage 0.6%.
3. PET Filament single yarn corresponding to sample 1, after annealing treatment: 300 m of yarn were annealed in hot air, under relaxed conditions at 220°C in a Benz equipment, for 1 hr.
4. PET Filament single yarn corresponding to sample 2, after annealing treatment: 300 m of yarn were annealed in hot air, under relaxed conditions at 220°C in a Benz equipment, for 1 hr.
5. PET tire cords (industrial sample): 114 tex f220 S 37 tpm (Tergal) × 4 S 152 tpm × 3 Z 98 tpm, stabilized sample (conditions of setting are unknown).
6. "100% Crystalline" sample obtained by progressive annealing of an amorphous yarn (see sample 12) and used as a 100% crystalline standard sample in the relative method. The annealing of the amorphous yarn was carried out under vacuum in a sealed tube from 60° to 230°C, with steps of 20°C. The sealed tube

was immersed in an oil bath, and each temperature step was maintained for 24 hr. The cooling was carried out according to an identical cycle from 230°C to room temperature. Density of this sample = 1.4295 g/cc (gradient column method).

Secondly, continuous preoriented yarns of very little crystallinity and corresponding to yarns produced for simultaneous draw texturization were studied:

7. POY (Preoriented yarn) spun at 2500 m/min: 363 dtex f30 (Tergal, Rhone-Poulenc-Textile), residual draft ratio 2.30.

8. POY spun at 3000 m/min: 301 dtex f30 (Tergal), residual draft ratio 1.90.

9. POY spun at 3300 m/min: 276 dtex f30 (Tergal), residual draft ratio 1.60.

10. POY spun at 3500 m/min: 259 dtex f30 (Tergal), residual draft ratio 1.55.

11. POY spun at 4000 m/min: 222 dtex f30 (Tergal), residual draft ratio 1.50.

12. "Amorphous" yarn collected under the spinneret while cold and considered as "amorphous standard" in the considered method; density of this sample = 1.3426 g/cc (gradient column method).

Methods

The examinations were carried out with an x-ray Rigaku RU 200 diffractometer with a rotating anode, under the following conditions: K_αCu (monochromatization by Ross filters and pulse height analyzer); 40 kV, 80 mA, focus 0.1 × 10 mm; Rigaku goniometer SG9 running in step-scanning mode with an increment of 0.1° in 2θ.

Taking into account the angular interval examined, the experiments were carried out in symmetrical transmission from 7° to 75° in 2θ and in symmetrical reflexion from 70° to 130° in 2θ. The experimental conditions relative to the sizes of the slits in the preparation of the sample were studied in such a manner that the connection of the diagrams in transmission and reflexion, as well as the ulterior standardization with respect to the theoretical curve, could give the best results. Several successive adjustments have led to the following conditions:

Symmetrical Transmission. Divergence slit 1/6°; analysis slit 0.6 mm; distance between sample and analysis slit 150 mm; sample thickness $t \simeq 1$ mm. The sample is prepared as a pellet, with a quantity of 0.800 g cut fibers 80 microns long (see below) under a pressure of 350 kg/cm^2 inside a rectangular sample holder of 2.0 × 1.8 cm. The samples prepared for examination in symmetrical transmission have $\mu t = 1.20$, where μ = linear absorption coefficient in cm^{-1}.

Symmetrical Reflection. Focalization conditions (diameter of goniometer 250 mm); divergence slit 1/2°; analysis slit 0.6 mm; sample thickness $t = 3$ mm. The sample is prepared by making 2.4 g cut fibers 80 microns long which are pressed inside a rectangular sample holder of dimensions 6 × 1.8 cm. Such samples have $\mu t \simeq 1.60$.

Preparation of Samples

The study of the crystallinity of fibrous materials requires the preliminary realization of a "global sample" in which all preferential orientation has been eliminated. This is generally obtained by cutting the sample and placing the cross sections in the most isotropic manner inside the sample holder. In order to avoid this kind of preparation, Ruland proposed an electronic process[15] for the spherical averaging of the x-ray fiber diagram. This device allows the determination of the crystallinity or even a profile analysis of the peaks to be made using the oriented fibers wound on a frame.

Unfortunately, many samples of industrial fibers are present in the form of short fibers, textured yarns, crimped fibers, etc., and are not very suitable for the realization of homogeneous windings and therefore not suitable for use in the device described by Ruland.

We have therefore retained the first solution, which consists in cutting the fibers with an automatic microtome. The microtome comprises mainly a vertical flywheel controlled by an adjustable-speed motor (Fig. 1). There are two cutting heads on the flywheel which pass before a razor blade which can be adjusted (Fig. 2). The cutting heads are formed mainly of a hollow cylindrical body plated with PFE, into which are pulled the yarns or fibers presented as strands. The movement of the fibers toward the cutting-head end, where the razor blade is placed, is brought about by a mobile piston which can move inside the body of the cylinder over a length adjustable from 20 μm to 160 μm. The programmed advance of the piston is assured by a cam system mounted on the driving shaft, a roller ring, and a starwheel. The cross sections obtained are collected in a small

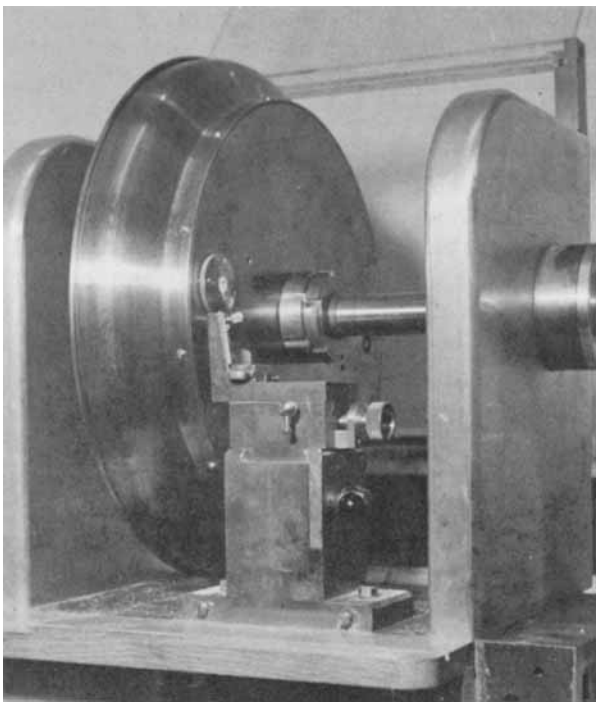

Fig. 1. General view of an automatic microtome to obtain cut fibers (length can be adjusted from 20 μ to 160 μ).

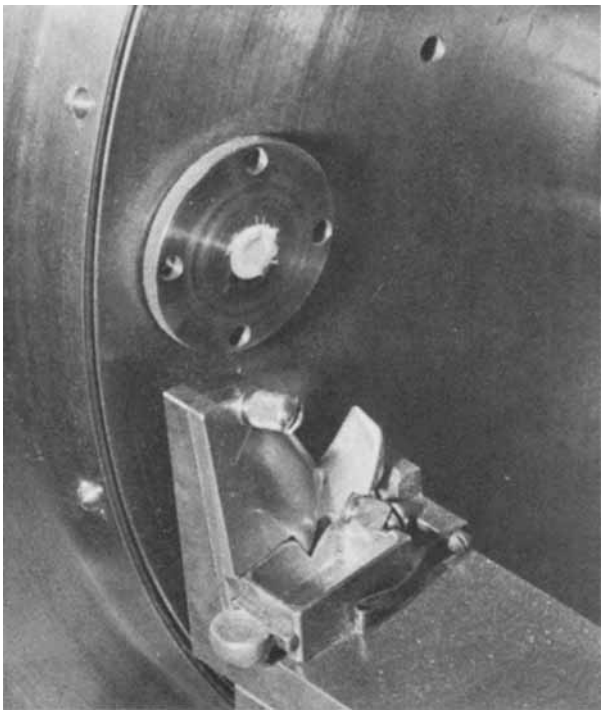

Fig. 2. Detail of the microtome at the level of a cutting head inside of which the sample is pulled. At each turn of the flywheel a piston can move inside the cylindrical part of the cutting head and push the yarn strand to the free end, where a razor blade is placed.

receptacle which is placed under the razor blade. They are then sifted, pelleted, and placed inside the sample holders previously described and arranged on convenient dies. The microphotograph of Figure 3 represents the appearance of cross sections obtained from settings from 60 to 80 μm. Careful pelleting of this powder gives samples in which practically all preferential orientation is eliminated.

In Figure 4, for example, the azimuthal scatterings are recorded at $2\theta = 17.5°$ i.e., at the PET peak (010), first with a bundle of parallel fibers arranged perpendicularly in front of the x-ray and second, on a sample of the same fibers cross sectioned and pelleted. It can be observed that despite the strong orientation of the fibers, it is possible to distribute the structural elements in a sample holder in an isotropic manner.

Treatment of Experimental Values

The experimental values were successively corrected with regard to the effects of air scattering, polarization, and absorption. The variable 2θ was transformed into

$$s = \frac{2 \sin \theta}{\lambda}$$

The corrected intensities were then standardized into an electronic unit by adjustment to the theoretical curve, summing up the contributions of the coherent and incoherent scatterings (Fig. 5).

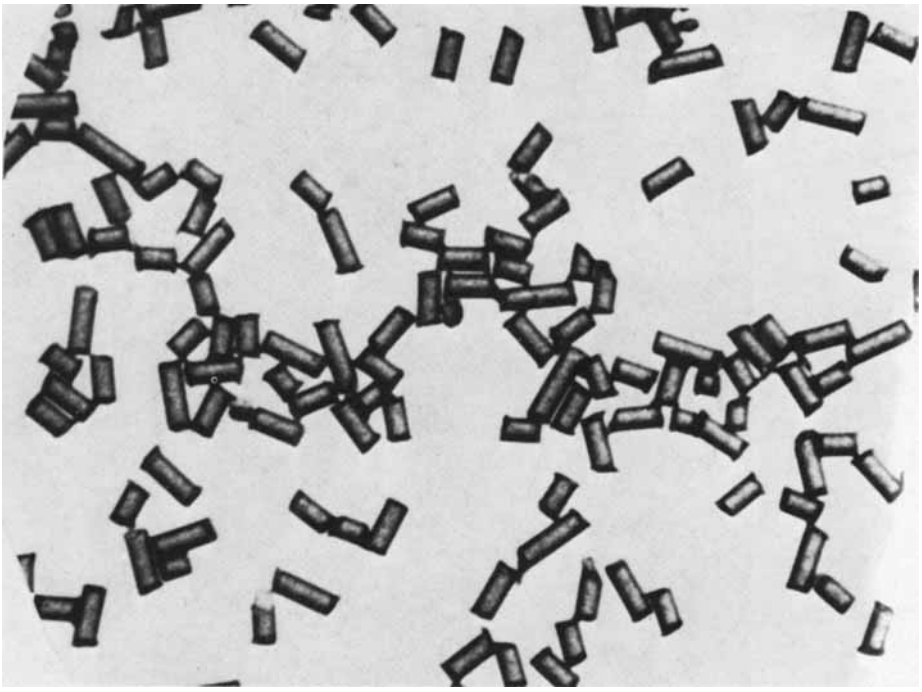

Fig. 3. Micrograph of fiber cross sections (cut length 60–80 μ).

The total scattering power of a given combination of atoms being independent of their mutual arrangement, the theoretical curve of the PET was calculated from the stoichiometric formula $(C_{10}O_4H_8)_n$, with

$$I_{(s)}(\text{coh}) = \bar{f}^2$$

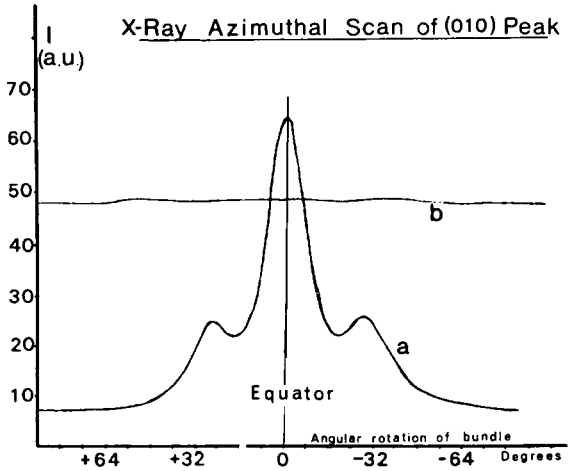

Fig. 4. Typical azimuthal scan curves carried out at the place of the (010) peak ($2\theta = 17.5°$): (a) bundle of parallel fibers put perpendicularly to the x-ray beam; (b) "powder" made of cut fibers. It can be ascertained that all preferential orientation is practically removed when a powder sample made of constant small cross sections is used.

and

$$\bar{f}^2 = \frac{\Sigma N_i \bar{f}_i^2}{\Sigma N_i}$$

where N_i = number of atoms of i kind in the stoichiometric formula.

The incoherent curve was calculated from

$$\frac{I_{(s)}(\text{incoh})}{Q(s\lambda)} = \frac{\Sigma N_i I_i}{\Sigma N_i}$$

where I_i = Compton scattering for the atom of i kind; $Q_{(s)}$ = Breit-Dirac coefficient = $(1 + (h\lambda/4mc)\, s^2)^{-3}$, with $h = 6.62 \times 10^{-34}$ mks units, $\lambda = 1.542 \times 10^{-10}$ m, $m = 9.11 \times 10^{-31}$ kg, and $c = 2.998 \times 10^8$ m/sec.

In order to obtain good standardization conditions of the experimental curve over the theoretical curve, Ruland and Vonk[7,8] strongly recommended the taking into account of the absorption discrepancy between the coherent and incoherent scatterings which become important for the wide angles of scattering. Because of this fact, corrections were successively made to the ratio of $I(\text{incoh})/I(\text{coh})$ in respect to the absorption effects in the sample, in the air, and in the Ross filters according to the method of calculation proposed by Ruland:

Absorption Within the Sample

Symmetrical Reflection. The sample is sufficiently thick to allow for the assumption that $\exp^{-2\mu t} \ll 1$. Therefore,

$$\left(\frac{I(\text{incoh})}{I(\text{coh})}\right)_{\text{obs.}} = \frac{\left(\frac{I(\text{incoh})}{I(\text{coh})}\right)_{\text{theor.}}}{1 + \frac{3h\lambda}{4mc} s^2}$$

Symmetrical Transmission.

$$\left(\frac{I(\text{incoh})}{I(\text{coh})}\right)_{\text{obs.}} = \left(1 - \frac{1}{2}\mu t \frac{6h}{mc\lambda} \cdot \frac{\sin^2\theta}{\cos\theta}\right) \left(\frac{I(\text{incoh})}{I(\text{coh})}\right)_{\text{theor.}}$$

Absorption in Air

$$\left(\frac{I(\text{incoh})}{I(\text{coh})}\right)_{\text{obs.}} = \left(\frac{I(\text{incoh})}{I(\text{coh})}\right)_{\text{theor.}} \exp^{-\mu' D} \frac{6h}{mc\lambda} \sin^2\theta$$

where D = distance in cm between the sample and the counter entry slit; and μ' = coefficient of the linear absorption of air = 0.0124 cm^{-1}.

Absorption by Balance Filters

$$\text{I(incoh)}_{\text{obs.}} = \text{I(incoh)}_{\text{theor.}} (\mu_B q \exp^{-\mu_B q t_A} - \mu_A \exp^{-\mu_A t_A}) \cdot 3t_A \frac{2h \sin^2\theta}{mc\lambda}$$

where t_A = thickness of Ni filter; $q = t_B/t_A$; t_B = thickness of Co filter; and μ_A

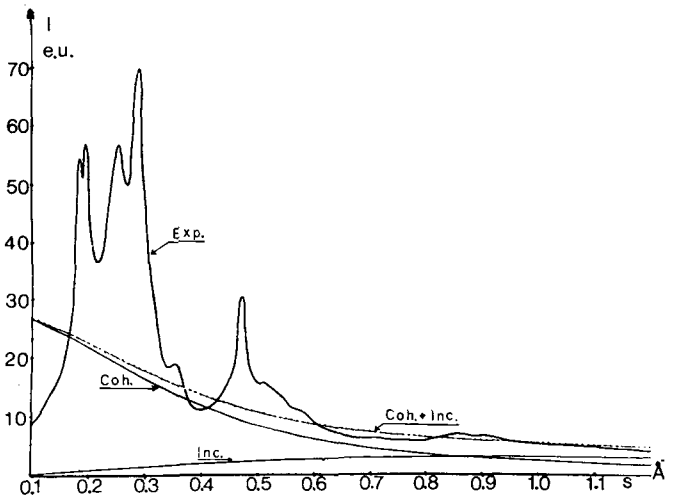

Fig. 5. Theoretical curves of scattered intensity by PET and experimental normalized intensity by PET fibers.

and μ_B = coefficients of linear absorption of Ni and Co. Taking into account the corrections made in this way and the recorded variations for the experimental intensities at wide diffraction angles, the standardization constant was calculated by comparing the integrals for the experimental and theoretical curves in an angular range from 0.85 to 1.20 in s. Figures 6 and 7 show plots of $s^2 I$ (in e.u. $Å^{-2}$) versus s (in $Å^{-1}$) for samples PET 4 and 6.

In the case of the relative method, the intensities being measured on a reduced angular range, and all corrections being made, the standardization is carried out by dividing the integral under the calculated curve by that under the characteristical curve of the amorphous standard.

RESULTS

Ruland's Method

Determination of Integration Intervals and Nomogram of K Values

The diagrams $s^2 I_{(s)}$ as a function of s drawn for the different samples studied, which varied widely in crystallinity, allowed the experimental definition of the finite integration zones such as relation (2) to be verified. These integration intervals are the following:

$$s_0 \text{ to } s_p = 0.1 \text{ to } 0.39$$

$$s_0 \text{ to } s_p = 0.1 \text{ to } 0.67$$

$$s_0 \text{ to } s_p = 0.1 \text{ to } 1$$

$$s_0 \text{ to } s_p = 0.1 \text{ to } 1.20.$$

It is therefore possible to calculate the K values on these intervals and for different k values. The results of the calculations are to be found in Figure 8. It can be verified, as Ruland has already shown with regard to polyethylene, that starting from a disorder function of spherical symmetry, the plots of K as a function of s_p^2 can be reduced to a series of straight lines.

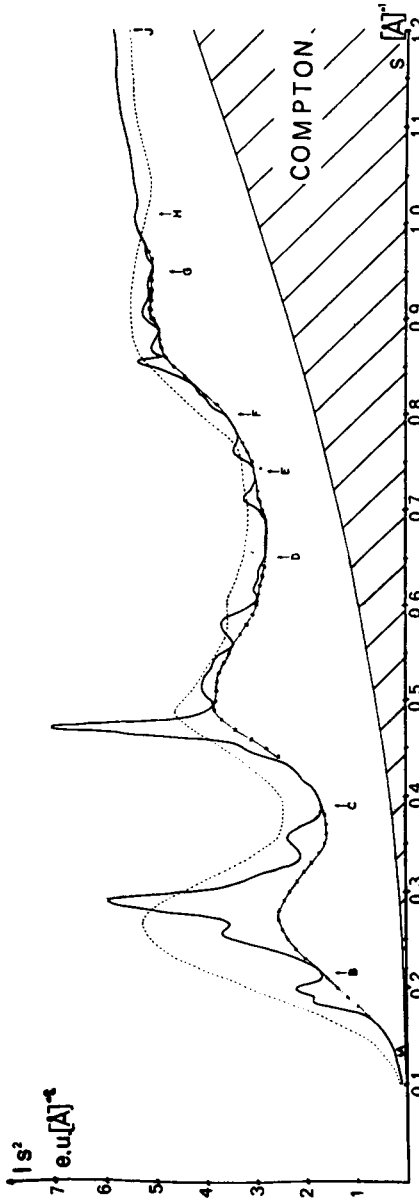

Fig. 6. Plot of $s^2I_{(s)}$ vs s for poly(ethylene terephthalate) fiber (sample 4): (---) $s^2I_{(s)}$ vs s for amorphous fibers sample (amorphous standard); (·····) amorphous background calculated, in the ranges A–B, B–C, C–D, etc., from the amorphous curve and a factor of proportionality c (see text).

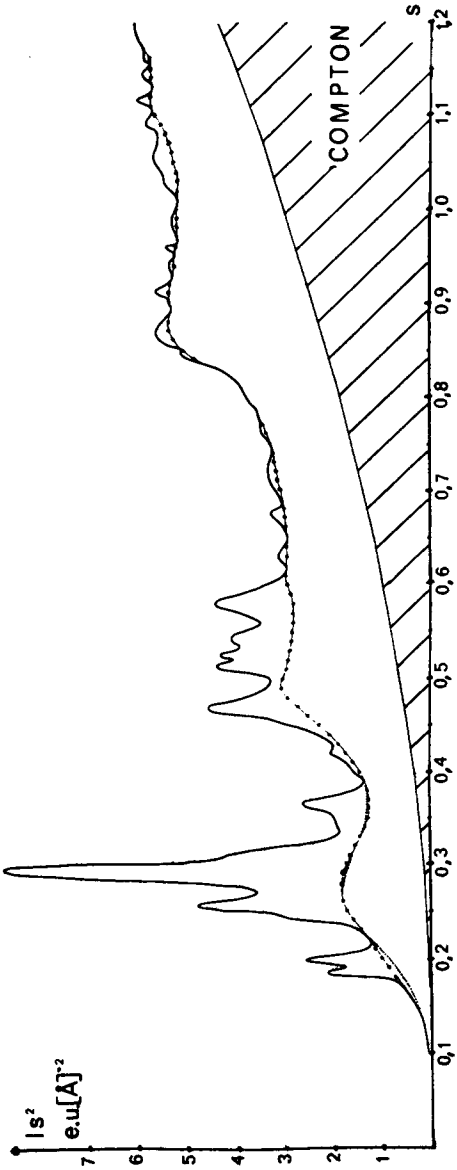

Fig. 7. Plot of $s^2 I_{(s)}$ vs s for PET fibers (sample 6, crystalline standard): (---) amorphous background calculated in the range $0.1 < s < 0.4$ following Chung and Scott's eq. (16):

$$Y = \frac{a}{x^2 + 1} + bx$$

where Y = background intensity, and $x = 2\theta$ value.

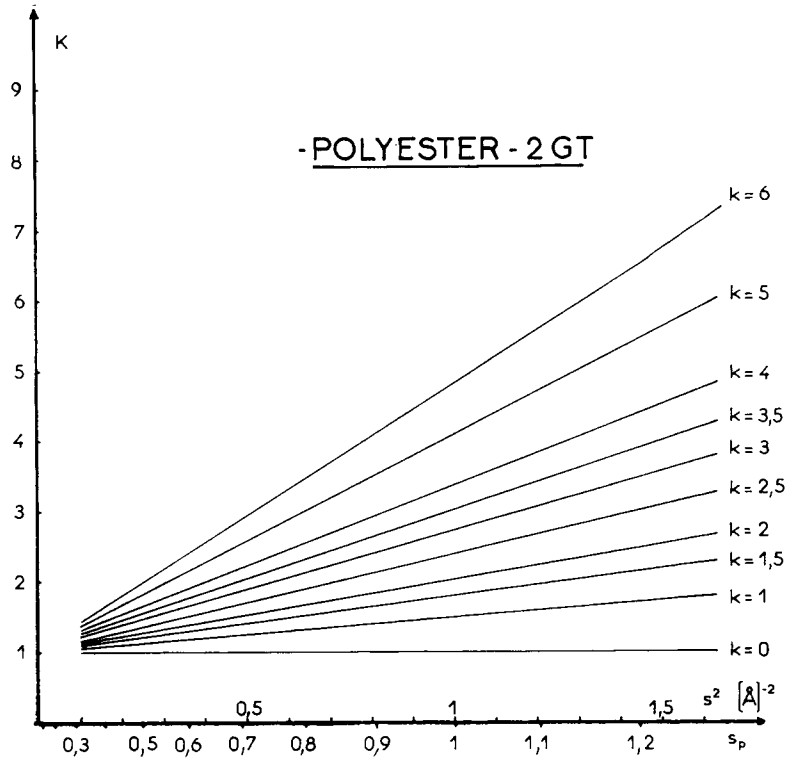

Fig. 8. Nomogram of $K(s_p^2 k)$ values for PET fibers, in the hypothetical ideal case where an isotropic disorder exists in the crystalline fraction of those fibers and calculated for the chemical composition $(C_{10}O_4H_8)_n$ and $s_0 = 0.1$.

Sketching of Amorphous Background Noise

Taking into account the relatively low crystallinity of the PET samples studied, which is evident at diagram level by a poor definition of the peak profiles and by their overlapping, it was necessary to pay the utmost attention to the drawing of the boundary line between the crystalline peaks and continuous diffusion. The most simple way of proceeding, taking the fibrous morphology of these samples into consideration was to take for reference the outline of the diagram characteristic of the "standard amorphous fiber" referred to in Figure 6.

In order to do this, the method proposed by Vonk was chosen. The hypothesis is made that the minimum intensity observed between two well-separated peaks on the diffraction diagram was due only to the amorphous fraction of the polymer, so that $s_1 < 0.13$, $s_2 = 0.215$, $s_3 = 0.39$, $s_4 = 0.65$, etc. Between these minima, i.e., the intervals s_1 to s_2, s_2 to s_3, etc., the curve of the background noise B is sketched according to the relation

$$I_B = I_{(\text{amorphous})} \times c$$

c being a factor varying linearly between the extreme values of intervals considered, such as c_1 for $s_1 = 0.13$, c_2 for $s_2 = 0.215$. The values of c_i are obtained from

$$c_i = \frac{I_i}{I_{(\text{amorphous})i}}$$

where I_i = measured intensity on the diagram of the studied sample for s_i, and $I_{(\text{amorphous})i}$ = measured intensity on the diagram of the amorphous sample for s_i.

In the diagram of Figure 7, relating to the "crystalline standard" in the first part of the integration region, the background noise is plotted first according to the above method and secondly according to the equation proposed by Chung and Scott[16]:

$$Y = \frac{a}{x^2 + 1} + bx$$

where Y = background noise intensity; x = angle in 2θ; and a, b are constants which can be determined from the known values of the intensities of the background noise, as, for example, at $2\theta = 20°$, where the maximum background noise is situated. It can be verified that the two methods lead to similar curves.

Expression and Discussion of Results

The results were grouped in Tables I and II. In examining the values of Table I, it can be verified that x_c for $k = 0$ drifts considerably according to the integration interval chosen. The values recorded for x_c and k in samples 1–5 appear to coincide perfectly with those found by Vonk[8] for nonfibrous morphology PET samples: $2.5 < k < 2.6$ and $0.34 < x_c < 0.44$. The "standard crystalline" sample shows, in fact, only a true crystallinity of 0.66. It can be ascertained also that any heat treatment which has a macroscopic effect of bringing about large free shrinkage is accompanied by an increase in crystallinity as well as in disorder factor. This is the case of samples 2, 3, and 5 in comparison with sample 1. On the contrary, any annealing treatment on a stabilized fiber, as in sample 3, leads only to a very slight increase in crystallinity but, above all, to a net decrease in the disorder parameter (see sample 4).

Without regard to the mechanisms involved during the shrinkage process, it is interesting to rate that, for a sample with high shrinkage ability (sample 1), annealing treatment produces not only an increase in the crystalline fraction and lattice imperfection but also a strong structural bipolarization (chain folding), as seen in the large change in small-angle intensity (Fig. 9). The intensity of the small-angle pattern is directly associated with the $\Delta\rho$ "electronic density" difference between the amorphous and crystalline areas. Besides, even if the fibers do not have any residual shrinkage capacity (sample 2), annealing treatment, which does not increase the degree of crystallinity to a great extent, produces nevertheless a large change in small-angle intensity (Fig. 10). Such a result could be explained by the decrease in the disorder parameter which has been found after annealing of a low-shrinkage capacity sample. The annealing treatment would, in that case, remove the structural distortions and leave a better delimitation at the level of the "amorphous–crystalline" interface and therefore a greater $\Delta\rho$ value.

Nevertheless, the results obtained from the "crystalline standard" seem to indicate that even extended annealing does not yield values of $k < 2.6$ which remain inferior to those characteristic of fibers slightly or not at all bipolarized ($k = 2.5$ for sample 1). This "limitation" of the order of annealed fibers could be inherent in the development of a lamellar crystallization with folded chains (structural perturbations at the level of molecular folds and chain ends).

TABLE I
Crystalline Fraction x_c in PET-2 GT Fibers as Function of k and Integration Interval

	Crystalline fraction x_c											
	Sample 1 (industrial yarn, shrinkage 8%)		Sample 2 (fixed industrial yarn, shrinkage 0.6%)		Sample 3 (annealed 1 hr at 220°C)		Sample 4 (annealed 1 hr at 220°C)		Sample 5 (fixed industrial ply yarn)		Sample 6 (crystalline standard)	
s_0–s_p Interval	$k = 0$[a]	$k = 2.5$	$k = 0$	$k = 2.9$	$k = 0$	$k = 2.8$	$k = 0$	$k = 2.6$	$k = 0$	$k = 2.9$	$k = 0$	$k = 2.6$
0.1–0.39	0.204	0.242	0.292	0.365	0.309	0.383	0.321	0.401	0.285	0.356	0.536	0.670
0.1–0.67	0.146	0.232	0.188	0.333	0.204	0.354	0.214	0.363	0.170	0.300	0.383	0.649
0.1–1	0.100	0.231	0.128	0.352	0.139	0.360	0.155	0.386	0.120	0.311	0.252	0.627
0.1–1.20	0.08	0.239	0.106	0.357	0.119	0.390	0.130	0.406	0.100	0.337	0.223	0.698
x_c Average		0.24		0.35		0.37		0.39		0.33		0.66

[a] When $k = 0$, no correction for distortion is taken into account for the calculation of the crystallinity value in eqs. (3) and (4). In that case, the crystallinity values are systematically lower than those obtained when a distortion parameter is considered, and the differences become greater in proportion as the intervals s_0–s_p increase.

TABLE II
Crystalline Fraction x_c in POY yarns as Function of k and Integration Interval

	Crystalline fraction x_c									
	Sample 7 (2500 m/min)		Sample 8 (3000 m/min)		Sample 9 (3300 m/min)		Sample 10 (3500 m/min)		Sample 11 (4000 m/min)	
s_{0-p} Interval	$k = 0$	$k =$	$k = 0$	$k = 1.5$	$k = 0$	$k = 1$	$k = 0$	$k = 1$	$k = 0$	$k = 1.7$
0.1–0.39	0		0.015	0.017	0.015	0.016	0.015	0.016	0.044	0.049
0.1–0.67	0		0.014	0.02	0.021	0.026	0.017	0.021	0.039	0.053
0.1–1	0		0.009	0.017	0.017	0.025	0.114	0.017	0.026	0.047
0.1–1.2	0		0.008	0.017	0.015	0.025	0.097	0.017	0.022	0.049
Average x_c		0		0.02		0.02		0.02		0.05

Concerning the results obtained in preoriented fibers, it appears that poor crystallization is initiated by spinning speeds between 2500 and 3000 m/min. Higher speeds in the order of 3000–3500 m/min, which approximately correspond to the industrial conditions for the production of these yarns, do not increase the crystalline fraction but seem, on the contrary, to increase the "perfection" of crystalline nuclei (decrease of k from 1.5 to 1). The appearance of a more important crystalline fraction is recorded for speeds of 3500–4000 m/min, as well as a greater disorder.

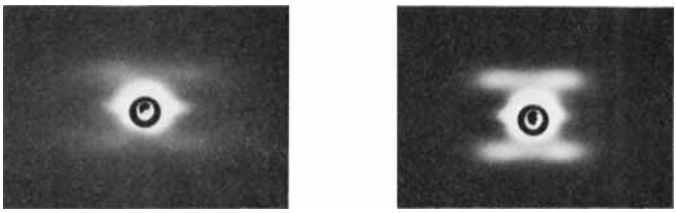

(a) (b)

Fig. 9. Small-angle diagrams of PET fibers. Nickel filtered CuK_α radiation, specimen-to-film distance 400 mm, fiber axis vertical: (a) intensity value 70 arbitrary units, sample 1 (industrial yarn, ability of shrinkage 8%); (b) intensity value 380 a.u., sample 1, annealed (without tension) 1 hr at 220°C.

(a) (b)

Fig. 10. Small-angle diagrams of PET fibers. Nickel-filtered CuK_α radiation, specimen-to-film distance 400 mm, fiber axis vertical: (a) intensity value 250 a.u., sample 2 (industrial yarn, ability of shrinkage 0.6%); (b) intensity value 480 a.u., sample 2, annealed (without tension) 1 hr at 220°C.

The hypothesis can be advanced that the crystalline nuclei created during spinning have a high degree of order and that the value of $k = 1$ for these yarns mainly shows the thermal disorder. Because of this fact, the effect due to the distortions of first and second order in fibers 1–6 would be two or three times that which would be due only to the thermal effect.

Relative Method

The crystallinity indexes measured according to this method are shown in Table III. They clearly indicate that according to the quality of the monochromatization of the incident beam, the crystallinity values differ as well as the classification of the samples according to their crystallization state. Taking into account that at $2\theta = 20°$ an appreciable fraction of the intensity is due to white radiation when only one Ni filtration is used and that the relative method does not take into account intensities other than those between 10° and 40° in 2θ, it seems necessary to conduct these examinations with a better monochromatization of the x-ray beam.

The classification of the I_c values obtained with Ross filters is identical to that of the x_c values. The correlation between the results of the two methods is excellent (Fig. 11), with a coefficient of 0.99. It is therefore possible, in a routine exercise, to determine the I_c according to the simple method and to carry out the transformation to x_c from the adjustment line of Figure 11. Obviously in a case like this, the x_c value will not be qualified by a disorder parameter. All the same, it seems useful to emphasize that the correlation is valid for extreme textile fibers, either of poor crystallinity or of relatively strong crystallinity. It would be suitable to establish the relationship between x_c an I_c for every kind of PET fibers before undertaking routine work.

TABLE III
Crystallinity Indexes Calculated According to the Relative Method

	Monochromatization by Ross filters and discrimination		K_αCu, Ni filtered and discriminated	
Samples	I_c, %	Validity coefficient $(1 - r^2)$	I_c, %	Validity coefficient $(1 - r^2)$
Sample 1 8% shrinkage	35.5	0.13	27.9	0.09
Sample 2 0.6% shrinkage	50.5	0.07	38.4	0.06
Sample 3 treated at 220°C	52.2	0.06	43.1	0.04
Sample 4 treated at 220°C	54.4	0.07	41.1	0.07
Sample 5 fixed ply yarn	43.3	0.09	31.4	0.10
Sample 7 POY 2500 m/min	2.1	0.86	4.8	0.62
Sample 9 POY 3300 m/min	3	0.80	5.4	0.54
Sample 10 POY 4000 m/min	8.5	0.22	4.9	0.38

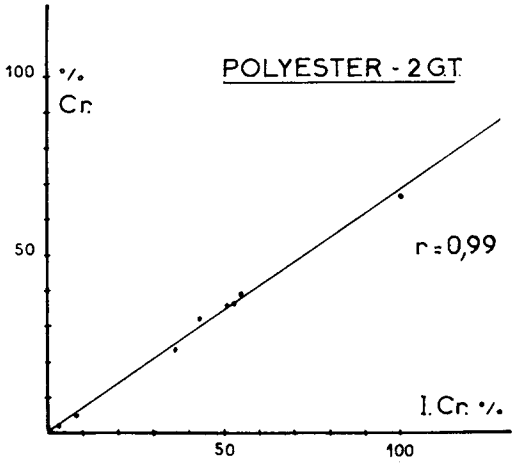

Fig. 11. Regression of Cr % (crystallinity following Ruland's method) on I_{cr} % (index of crystallinity following a relative method), for PET fiber samples.

The indexes of crystallinity were also determined according to Dumbleton's method.[17] This method is a very simple one and could be easily used in routine control: here, distortions are not considered. The results obtained appear in Table IV. It can be seen that the values of crystallinity index I'_c considerably change according to whether the x-ray beam monochromatization is good or not and intensity values are corrected or not. A relatively good agreement (same classification) exists for the different samples between x_c and I'_c values only when I'_c is calculated from corrected intensities. Nevertheless, in spite of the fact that

TABLE IV
Crystallinity Indexes I'_c Calculated According to Dumbleton's Method.[a] Lattice Distortions Not Considered

Samples	I'_c, % Observed intensity values, Ni filtration	I'_c, % Monochromatization by Ross filters, corrected intensities
Sample 1		
8% shrinkage	46.8	47.1
Sample 2		
0.6% shrinkage	53.4	57.9
Sample 3		
treated at 220°C	56.1	57
Sample 4		
treated at 220°C	53.7	58.5
Sample 5		
fixed ply yarn	48.4	50.5
Sample 6		
crystalline standard	83.3	74

[a] Dumbleton's x-ray crystallinity is defined as

$$I'_c = \left(1 - \frac{A}{A_{100}}\right) \times 100$$

where A = ratio of the intensities (above the background) at 2θ = 1h° and 2θ = 28.5° for any given sample, and A_{100} = value of this ratio for the amorphous sample. The background at any point of the x-ray diagram is obtained by linear interpolation between the points 2θ = 5° and 2θ = 38°.

distortions are not considered, the Dumbleton crystallinity indexes are unexpectedly higher than the corresponding x_c values. This could be explained by the different ways of sketching the amorphous background in the two methods.

Estimation of Mesophase Fraction in Preoriented Yarns (POY)

The preoriented yarns, even though not very crystallized, have nevertheless a phase relatively well oriented along the axis of the fiber, as illustrated in the x-ray diagram of Figure 12 relative to a yarn preoriented at 2500 m/min. Such samples are of a certain interest because the estimation of this oriented part responsible for the anisotropy of the visible scatterings on the x-ray pattern could lead to the isolation of an intermediate mesophase fraction between amorphous and crystalline. The orientation of this intermediate phase is therefore responsible for the difference in the intensity distribution, which can be recorded for example between a radial scan carried out on the equator and another on the meridian. In Figure 13, we have superposed such diagrams recorded on 2500 m/min POY presented perpendicularly to an x-ray beam in the form of windings ($\mu t \simeq 0.50$). The intensity differences $(\Delta I)_{(2\theta)i}$ are above all visible in the ranges of 15°–30° in 2θ and 40°–45° in 2θ, the first corresponding to the equatorial "mound," the second to a meridional "mound." The azimuthal scans are carried out this time by setting the counter at different given angles in the two above ranges, and by rotating the sample in its plane, this allowing the recording of the azimuthal intensity profile of the equatorial and meridian patterns.

The azimuthal breadth of the diffusion rings was estimated from the angle at 50% intensity breadth $\beta(2\theta)_i$ (Fig. 14). The hypothesis is formed that the

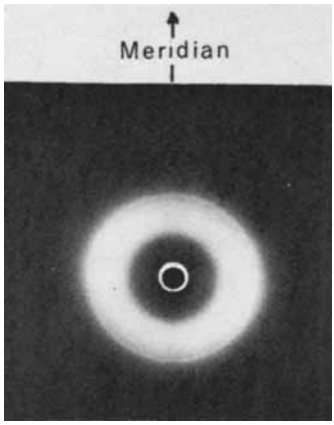

Fig. 12. X-Ray diagram of PET preoriented yarn, spun at 2500 m/min. No crystalline peak is visible on such a diagram; nevertheless, it is possible to ascertain on the equator of the amorphous halo an increase of the scattered intensity.

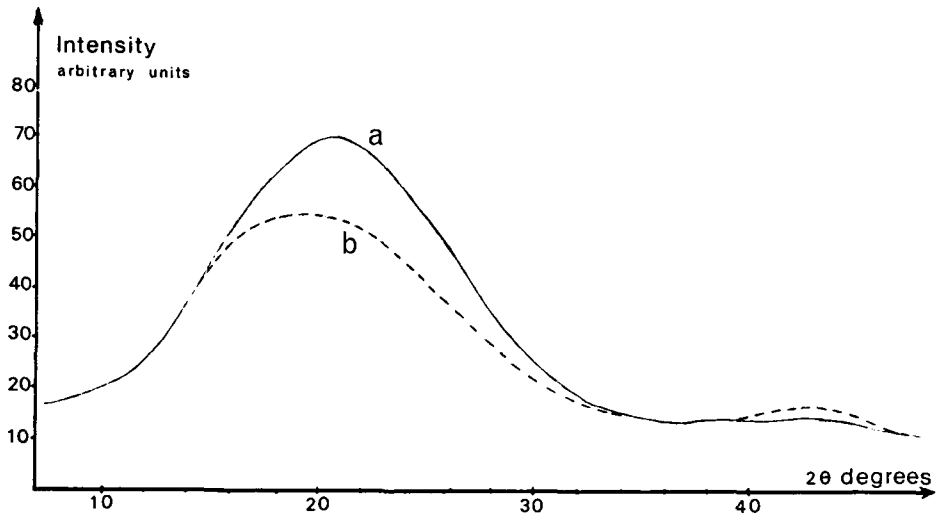

Fig. 13. Plot of scattered intensity vs 2θ, recorded under the same experimental conditions for a POY (2500 m/min) wound on a frame and put perpendicularly to the x-ray beam: (a) equatorial scan; (b) meridional scan. The discrepancies between the two scans, particularly inside the angular ranges $15° < 2\theta < 30°$ and $40° < 2\theta < 45°$, account for the anisotrope scattering due to the existence of an oriented mesophase fraction.

values $\Delta I_{(2\theta)_i}$ recorded for an anisotropic sample would become

$$(\Delta I)'_{(2\theta)_i} \simeq \frac{(\Delta I)_{(2\theta)_i} \times \beta(2\theta)_i}{180}$$

if the sample were examined under isotropic presentation (powder).

The values $(\Delta I)'_{(2\theta)i}$ thus calculated were directly sketched on the diagram recorded this time on an isotropic sample of $\mu t = 0.49$, under experimental

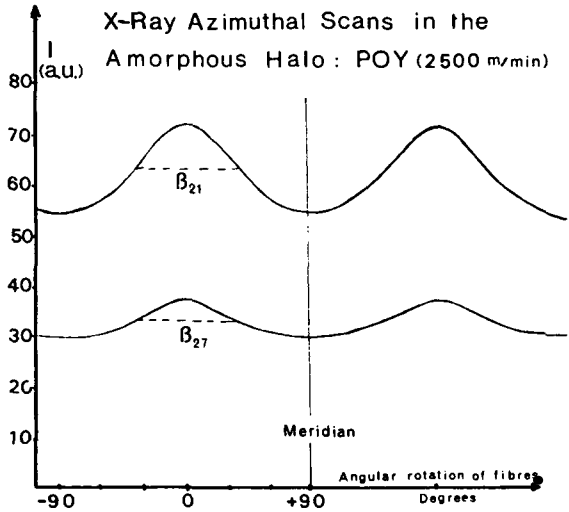

Fig. 14. Results of azimuthal scans carried out at the level of the equatorial intensity reinforcements of the amorphous halo ($2\theta = 21°$ and $2\theta = 27°$). Sample: POY spun at 2500 m/min. The azimuthal spread of the scattering pattern was measured by the breadth at 50% intensity (β).

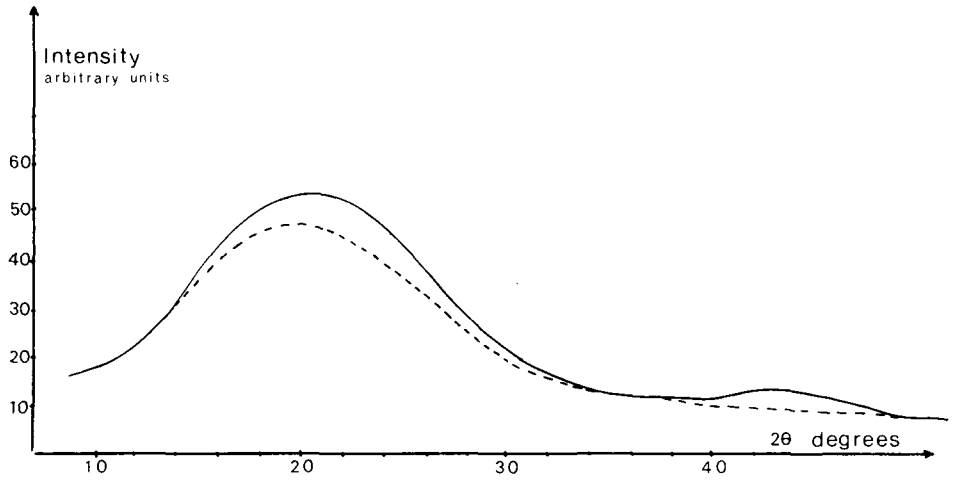

Fig. 15. Plot of scattered intensity vs 2θ, for POY spun at 2500 m/min. Powder sample made of cut fibers (isotrope sample). It is possible to directly compare this curve with those of Figure 13. All the curves were recorded under identical conditions. The absorption coefficients of the samples were similar: $\mu t = 0.49$ (powder); $\mu t = 0.50$ (wound yarn). The dotted curve obtained after deduction of an oriented mesophase could be more characteristic of the diffusion shape of a "real amorphous" sample.

conditions identical to those chosen for the parallelized sample (see Fig. 15). The appearance of the new curve obtained in this way, after deducting the oriented mesophase, would therefore be more characteristic of an "amorphous phase." It was drawn again, in keeping with the proportions, on the plot s^2I versus s.

This operation carried out on POY 2500 and on POY 3300 led to very similar "real amorphous" curves (Figs. 16 and 17). It is interesting to note (Fig. 17) that, at least in the angular interval $s = 0.1$ to $s = 0.4$, the appearance of this "calculated amorphous" curve is very like that obtained from a pulverulent amorphous, reference GY, of nonfibrous morphology and kindly supplied by R. Chung.[16]

The crystallinity calculations carried out again in reference to this new background noise enable the value x_c' to be defined as

$$x_c' = x_c + \text{mesophase}$$

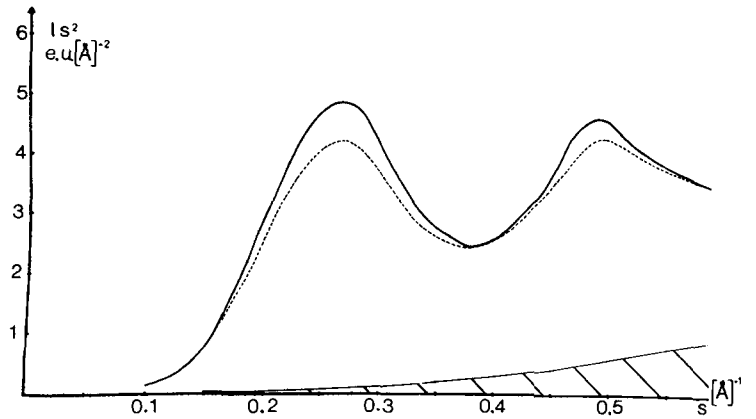

Fig. 16. Plot of $s^2I(s)$ vs s for a POY (2500 m/min) sample. The trace of the "real amorphous" was drawn again (dotted line), in keeping with the proportions, from those of the curves of Figure 15.

Fig. 17. Plot of $s^2I(s)$ vs s for a POY spun at 3300 m/min. Cross-sectional area corresponds to the crystalline fraction; it was drawn in reference to the "amorphous standard fiber" curve (see Fig. 6): (- - -) amorphous background calculated by deduction of an oriented mesophase; (···) curve of $s^2I(s)$ vs s, sketched in the angular range of $0.1 < s < 0.4$, for a pulverulent amorphous sample (nonfibrous morphology).

where x_c = crystalline fraction previously calculated in reference to "amorphous with fibrous morphology." The respective evaluation of x_c and of the mesophase fraction as a function of spinning speed is seen in Table V. It seems, therefore, that the initial crystallization of the polymer under the spinneret is detrimental to the mesophase fraction, which progressively diminishes in order to attain a slightly constant value for speeds from 3300 to 3500 m/min.

CONCLUSIONS

The choice of a corrective function D of spherical symmetry obviously imposes effects of isotropic disorder which do not represent very much the real structure of fibrous polymers in which the thermal motions and the network defects displace the atoms mainly in one direction, perpendicular to the axis of the chains. More rigorous calculations would thus impose taking into consideration a function of radial symmetry. In this case the calculation of the corrective function would be[18]

$$K = \frac{\sum_h |F_h^2|}{\sum_h |F_h^2| \exp^{-s_h k s_h}}$$

where F_h = structural factor of the unit cell for the reflexion $h(hkl)$.

The calculations made by Ruland[18] in the case of polyethylene showed that the crystallinity values are a little higher, taking into consideration an anisotropic disorder function rather than an isotropic disorder. This reminder being given, it can nevertheless be said that the transposition of Ruland's method for semicrystalline PET fibers seems interesting in many ways.

1. First, taking a disorder function into consideration, the "apparent" crystallinity is transformed into "real crystallinity," to which is associated a disorder parameter. In the light of these results obtained in the present study, it would seem that the structural disorder due to the distortions is two or three times more important than the thermal disorder.

2. The heat treatments which are accompanied by shrinking of the fibrous sample are the cause of an increase in crystalline fraction but leave very important distortions. On the contrary, the annealing treatments carried out on already stabilized fibers result in the disappearance of the distortions without any great increase in crystallinity. Each of these transformations could explain the changes in intensity of the small-angle diffraction diagram.

TABLE V
PET Preoriented Yarns: Respective Evaluation of the Crystalline (x_c) and Oriented Mesophase Fractions as a Function of the Production Speed

Sample	x_c	Oriented mesophase
POY 1000 m/mn	0	0.13
POY 2500 m/mn	0	0.13
POY 3000 m/mn	0.02	0.12
POY 3300 m/mn	0.02	0.10
POY 3500 m/mn	0.02	0.09
POY 4000 m/mn	0.05	0.09

3. It is possible to correlate, with a high validity coefficient, the crystallinities obtained according to Ruland's method and the crystallinity indexes calculated according to the relative method, under the condition, however, that rigorous experimental conditions be used.

4. To sum up, the study of the new preoriented yarns allowed the observation of the appearance of slight crystallinity in yarns produced at a speed of at least 3000 m/min.

The calculations carried out successively taking into consideration two levels of the background noise, one characteristic of an amorphous model with fibrous morphology, the other of pulverulent amorphous model, have permitted the estimation of an intermediate oriented mesophase between the amorphous and crystalline state. This mesophase, which corresponds in the x-ray POY diagram to the intensity reinforcements in the amorphous halo, appears as soon as the spinning speed is 1000 m/min; it then diminishes to the benefit of the crystalline fraction.

Such an operation, in the case of crystalline samples, does not give any mesophase fraction. On the contrary, it is interesting to note that the simultaneous drawing–texturizing of POY yarns results in fibers moderately crystallized in which there is a mesophase fraction (unpublished results).

References

1. W. L. Lindner, *Polymer,* **14,** 9 (1973).
2. G. Jellineck, W. Ringens, and G. Heidemann, *Ber. Bunsenges. Chem.,* **20,** 564 (1970).
3. P. Bouriot, J. Jacquemart, and M. Sotton, *Bull. ITF,* **6,** 21 (1977).
4. J. H. Dumbleton, *J. Polym. Sci. A-2,* **6,** 795 (1968).
5. A. M. Hindeleh and D. J. Johnson, *Polymer,* **13,** 27 (1972).
6. A. M. Hindeleh and D. J. Johnson, *Polymer,* **15,** 697 (1974).
7. W. Ruland, *Acta Crystallogr.,* **14,** 1180 (1961).
8. C. G. Vonk, *J. Appl. Crystallogr.,* **6,** 148 (1973).
9. B. Fauchet, L. Slobodkin, and R. Perret, *C.R. Acad. Sci. Série C, Paris,* **280,** 101 (1975).
10. A. Viswanathan and V. Venkatakrisnnan, *J. Appl. Polym. Sci.* **13,** 785 (1969).
11. J. H. Wakelin, H. S. Virgin, and E. Crystal, *J. Appl. Phys.,* **30,** 1654 (1959).
12. W. O. Statton, *J. Appl. Polym. Sci.,* **7,** 803 (1963).
13. N. B. Patil, N. E. Dweltz, and Radhakrishnant, *Text. Res. J.,* **32,** 460 (1962).
14. R. Hagege, J. Jacquemart, and M. Sotton, Colloque G.F.P., Les Polymères en Papeterie, Grenoble, October 16–17, 1975.
15. W. Ruland and A. Dewaelhegus, *J. Sci. Instrum.* **44,** 236 (1967).
16. F. H. Chung and R. W. Scott, *J. Appl. Crystallogr.,* **6,** 225 (1973).
17. J. H. Dumbleton and B. B. Bowles, *J. Polym. Sci. A-2,* **4,** 951 (1966).
18. W. Ruland, *Faserforsch. Textil-Tech.,* **18,** 59, 63 (1967).

Received March 14, 1977
Revised June 2, 1977